

Structural Observation on Wood and Bamboo by X-ray*

Takaya NOMURA** and Tadashi YAMADA**

Abstract—Correlation of the quantitative change of the cell wall components and its structural properties during growth of Akamatsu and Mōsō bamboo has been investigated by using X-ray. The results are as follows.

(1) The micell angle of the cell wall of Mōsō bamboo distributed scatteringly near the ground height and the top, but in the middle part the distribution is in a close range around the b-axis.

(2) In Akamatsu wood, the distribution of the micell angle of the spring wood was wider than that in the summer wood.

(3) Mean micell angle calculated from (040) arc was sharper than the one calculated from (002) arc by $3^{\circ}\sim 5^{\circ}$, and it seemed that there is a linearity between the values of the two arcs.

(4) It may be said that the micell angle depends greatly on the cell length, and the relationship between the micell length and the mean micell angle corresponds to the relationship between the tracheid length and the mean micell angle.

(5) No significant difference is observed from the ground to the top of Moso bamboo for the degree of crystallinity.

Introduction

Changes of physical properties of the plant stem during growth have seldom hitherto been studied, and it is very important to elucidate their changing mechanism during formation of plant stems.

For the purpose to investigate the physical and chemical properties of the plant stem in the growing process the bamboo has mainly been used, because the bamboo grows rapidly, so that the samples by which the change of physical and chemical properties at each stage of the growing process enable to investigate are easy to get.

Mōsō bamboo (*Phyllostachys heterocycla form.*) grows to full size within about 2 months, but it needs about 3 years for its complete maturation. The main structure, composed of cellulose fibers, have been completed at an earlier period, and then the cell-wall growth and lignification proceed gradually.

In this paper the micell size, the distribution of micell angle, the mean micell

* Presented at the 20th and 21st Meetings of Japan Wood Research Society, held at Tokyo, Autumn 1970 and at Nagoya, April 1971 respectively.

** Division of Wood Physics.

Table 1. X-ray measurement conditions.

	Voltage (kV)	Current (mA)	c. p. s.	Time constant	Scanning speed	Chart speed	Divergence slit	Receiving slit	Angular velocity
A	60	100	400~8000	2 sec	1°/min	10 mm/min	1 mm pinhole	2×3 mm	2°/min
B	60	100	800~8000	2	1	10	1	2×3 mm	2
C	50	80	4000	2	1	10	1/2 degree	1/2 degree	
D	50	80	4000	2	1	10	1/2	1/2	
E	50	80	4000	2	1	10	1/2	1/2	

A: The distribution of the micell angle, the mean micell angle and micell length from (040) arc of Mōsō bamboo.

B: The distribution of the micell angle, the mean micell angle and micell length from (040) arc of Akamatsu wood.

C: The micell width of Mōsō bamboo.

D: The micell width of Akamatsu wood.

E: Degree of crystallinity of Moso bamboo.

X-ray diffractometer: Rota flex (Rotating anode X-ray generator, Rigaku Denki Co., Ltd.)

Target: Cu K α . Filter: Ni.

measured. In making measurements of crystalline or "X-ray" orientation in cellulosic fibers, the aim was to obtain the distribution of angles made by the long or b-axes of crystallites with the fiber axis. For this purpose, the intensity of X-ray diffraction should be measured as a function of azimuth along a "diatropic" or meridional diffraction arc, such as the relatively intense (040) reflection. The distribution of (040) lattice plane of a meridian is shown in Fig. 1.

The scintillation counter was held in the horizontal plane, set with an angle of $2\theta=34.8^\circ$ for the incident beam, which emerges through the pinhole collimator. The rotation axis of the face plate was inclined with an angle of $\theta=17.4^\circ$ to the incident beam which passes through the center of the area where the X-ray beam is projected to the sample. Based on the revolution angle and the intensity distribution the distribution of the micell orientation D was calculated from equations 1, as shown in Fig. 1.

$$D = \sin \alpha \cdot I \quad (1)$$

$$\cos \alpha = \cos \theta \cdot \cos \varphi_i \quad (\alpha > \theta)$$

$$\cos \alpha = 1 - (1 - \cos \varphi_i) \cos^2 \theta \quad (\alpha < \theta)$$

The X-ray measurement condition are shown in Table 1. The mean micell angle were obtained by Cave's method from the angular width of (002) diffraction arc.

Micell width and micell length

The micell width and micell length were measured with respect to the LT and LR faces for Mōsō bamboo, and the LR face for Akamatsu wood. The micell width was calculated from the (002) diffraction breadth on the paratropic plane by the SCHERRER'S equation. It is a question if the SCHERRER'S equation is to be able to apply for the decision of the crystalline dimension of the natural fiber. In this experiment, B_0 , observed diffraction peak breadth at half-maximum intensity was used instead of β , the pure diffraction broadening in the SCHERRER'S equation, as an index of crystalline dimension.

$$D = K\lambda / \cos \theta \cdot B_0$$

B_0 : observed diffraction peak breadth at half-maximum intensity.

θ : Bragg angle

λ : X-ray wave length in angstrom units ($=1.54 \text{ \AA}$)

K : crystallite-shape constant ($=0.9$)

D : mean crystallite dimension normal to diffracting planes.

The micell length was also calculated from the (040) diffraction arc on the diatropic plane.

Degree of crystallinity

Each sample of Mōsō bamboo was crushed into powder with 100~200 mesh. The powder was dried over the phosphorus pentoxide *in vacuo* (10^{-3} mmHg) at room temperature. Five hundred mg of the dried powder was taken, pressed into a tablet under the pressure of 400 kg/cm², are used for the measurement of crystallinity. The X-ray measurement condition is shown in Table 1.

Results and Discussion

Diffraction of micell angle and mean micell angle

The distribution curves of micell angles of Mōsō bamboo are shown in Figs. 2 a~2 e. In the first joint of the bamboo the distribution curves were scattered broadly around the b-axis, and the mean micell angles were 8 to 15 degrees. However, the micell angle of 9 th, 24 th and 30 th joint was distributed closely around the b-axis, and the mean micell angle was 6 degrees. In 50 th joint there was a large difference between the distribution of micell angles in the outer epidermis side and the inner epidermis side (Fig. 2 e). These differences are noteworthy in studying the structure of the bamboo in relation to physical properties of the cell wall.

The mean micell angle of each joint is shown in Fig. 3. The mean micell angle decreased remarkably from the first joint to the 9th and remained nearly

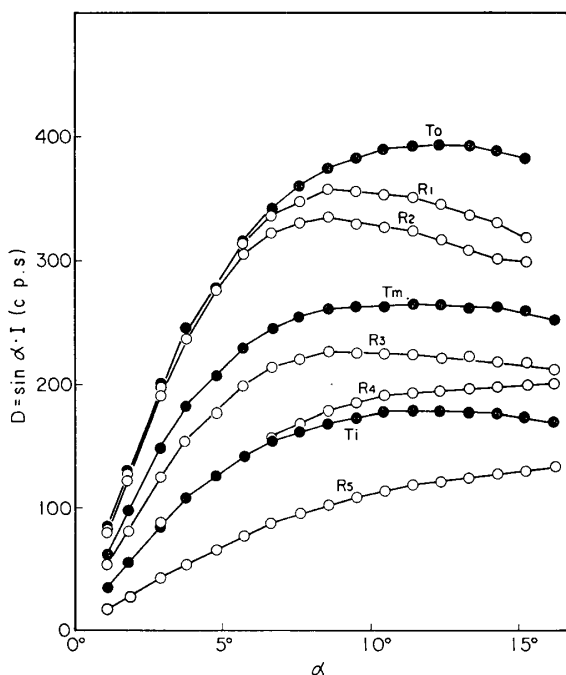


Fig. 2 a. Distribution (D) of the angle of micellar orientation of first joint of Mōsō bamboo.

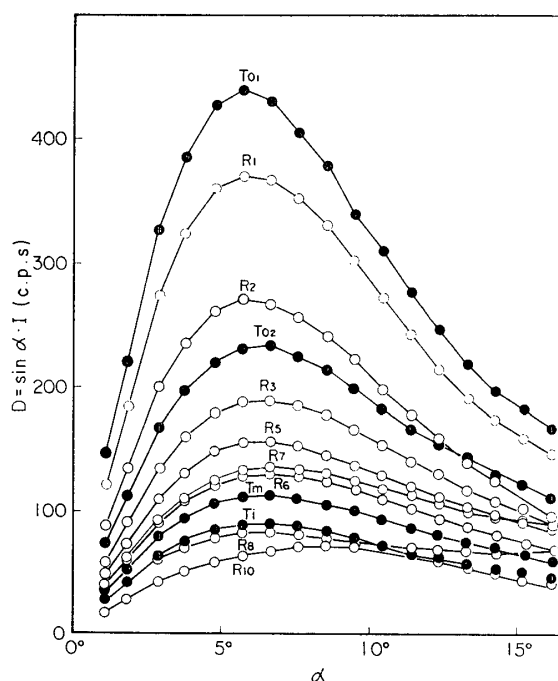


Fig. 2 b. Distribution (D) of the angle of micellar orientation of the 9th joint of Mōsō bamboo.

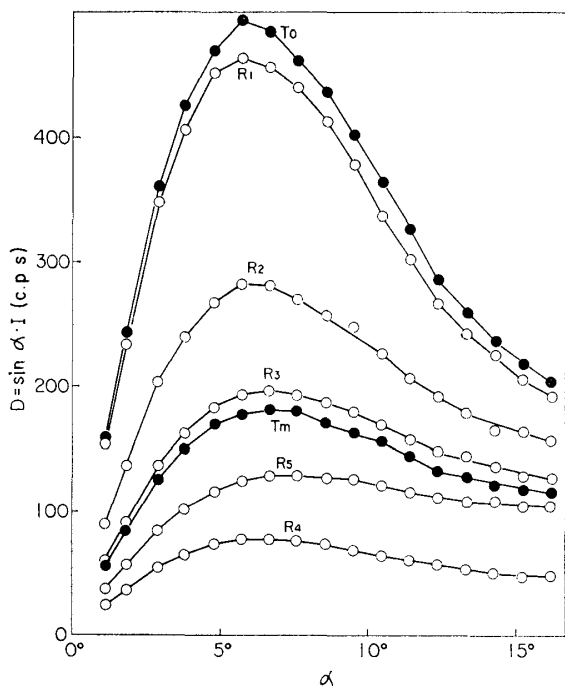


Fig. 2c. Distribution (D) of the angle of micellar orientation of the 24th joint of Mösö bamboo.

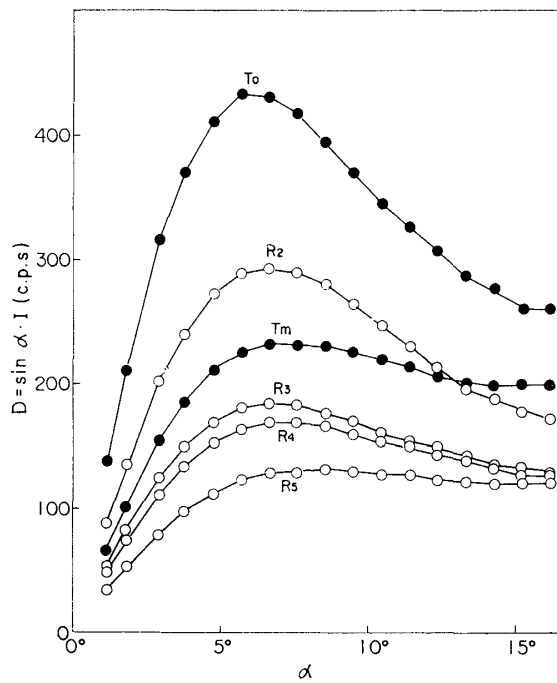


Fig. 2d. Distribution (D) of the angle of micellar orientation of the 30th joint of Mösö bamboo.

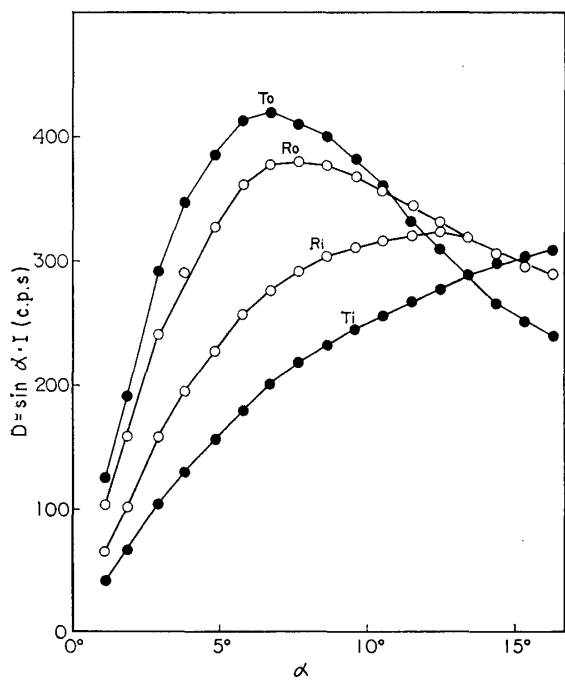


Fig. 2e. Distribution (D) of the angle of micellar orientation of the 50th joint of Mösö bamboo.

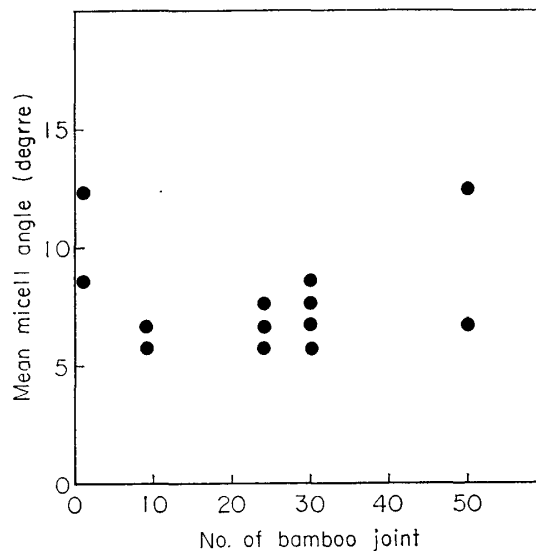


Fig. 3. Mean micell angle of Mösö bamboo.

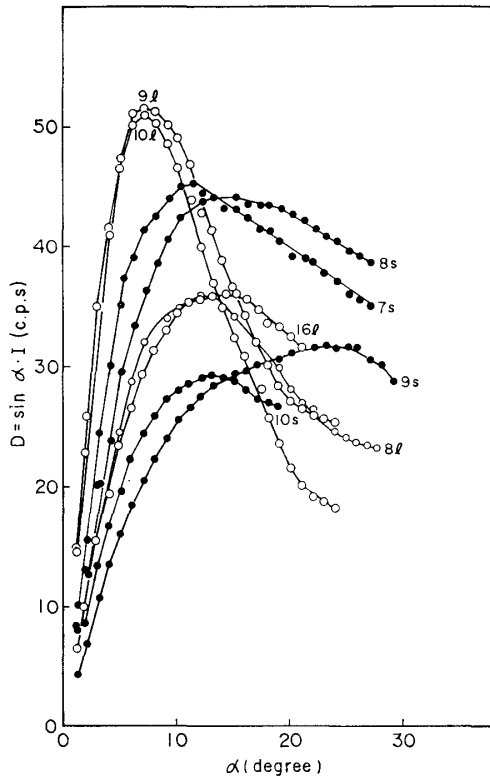


Fig. 4 a. Distribution (D) of the angle of micellar orientation of Akamatsu wood.

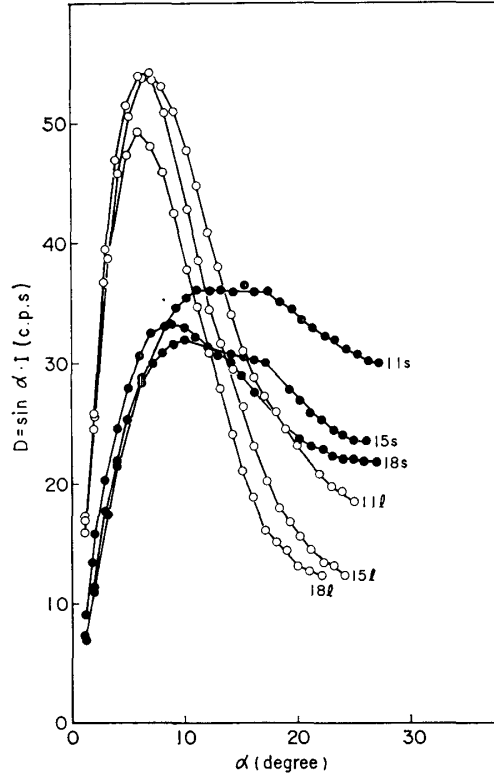


Fig. 4 b.

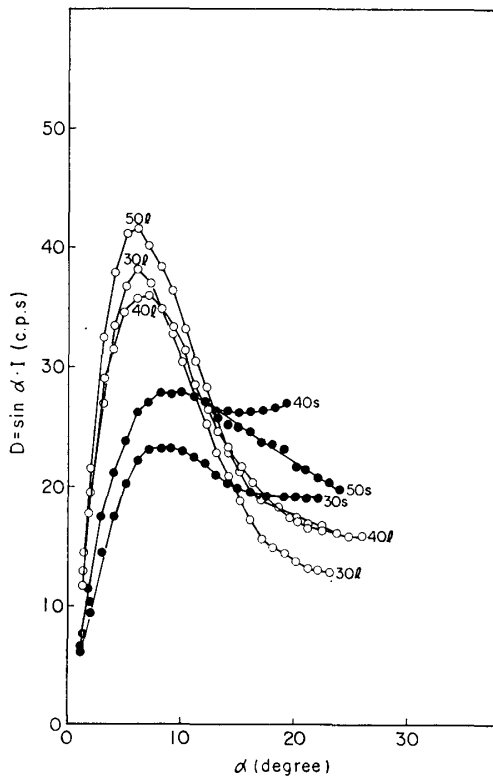


Fig. 4 c.

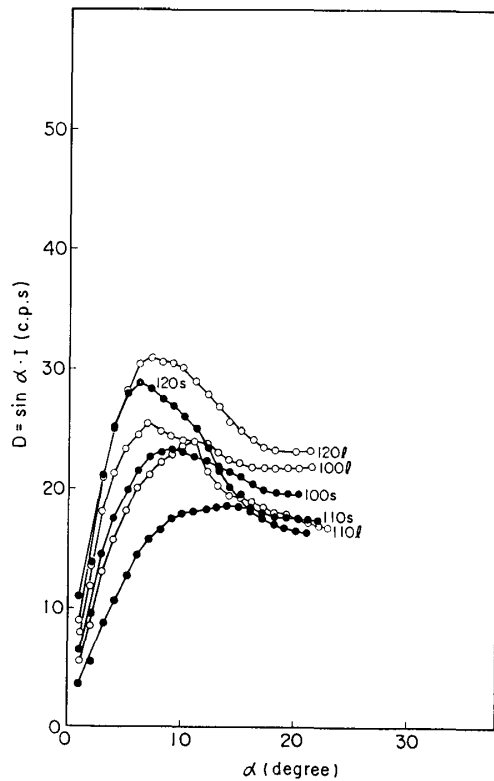


Fig. 4 d.

constant from the 9th to 30th, and then increased slightly in the 50th joint. In comparison with the mean micell angle in the outer epidermis side with that in the inner epidermis side in the 50th joint, the former was smaller than the latter.

The distribution curves of Akamatsu wood are shown in Figs. 4 a~4 d. The distribution of the micell angle of the springwood was wider than that of the summer wood. It is interesting to note that significant differences were observed in the distribution of the micell angle from the pith to the bark among annual rings, and that the environmental factors have little effect on the process of formation of the micell of the trunk.

The mean micell angle from the pith to the bark of Akamatsu wood is shown in Fig. 5. The angle decreased fairly from the pith to the 12th-13th annual rings and then remained nearly constant near the bark. However, it increased slightly near the bark. Comparison of the spring wood with the summer wood indicated the same pattern as mentioned above and that the scattering degree of these values was wider in the spring wood than in the summer wood.

Fig. 6 shows the mean micell angle in the spring wood and the summer wood of Akamatsu by the CAVE's method. It was found that the mean micell angle

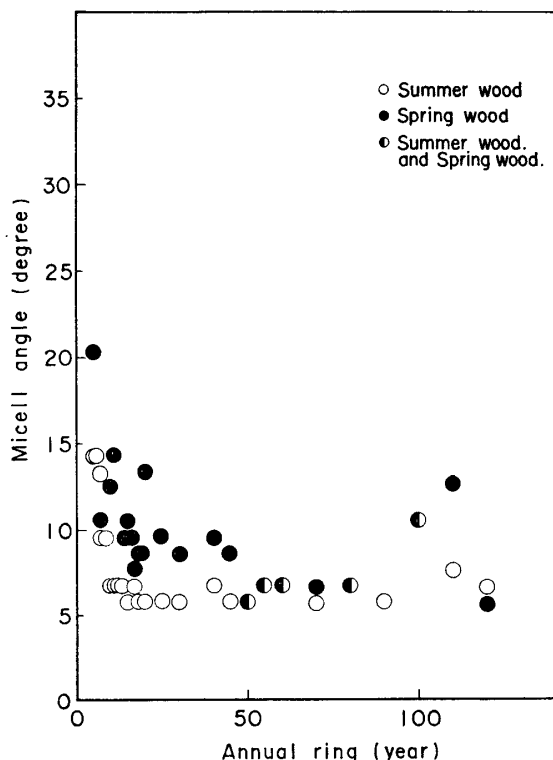


Fig. 5. Mean micell angle of Akamatsu wood from pith to bark from (040) arc.

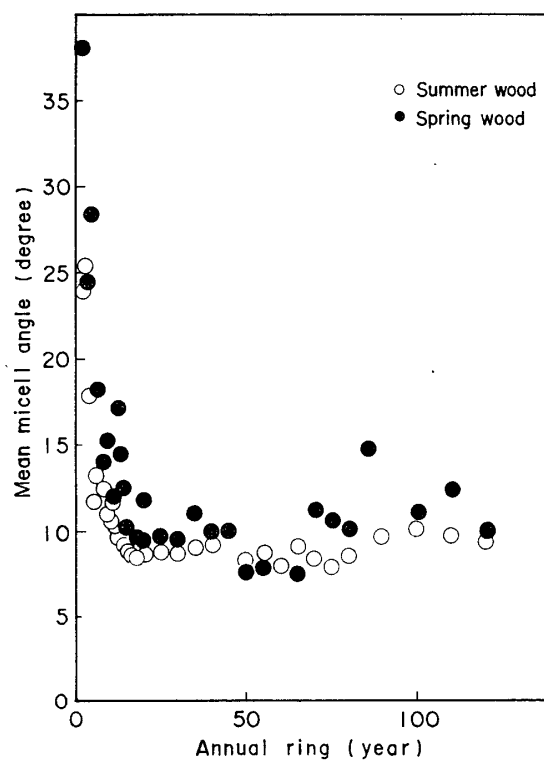


Fig. 6. Mean micell angle of Akamatsu wood from pith to bark by CAVE's method.

calculated from (040) arc was sharper than the one calculated from (002) arc by $3^{\circ}\sim 5^{\circ}$. The correlation between the mean micell angle from (040) diffraction and that from (002) diffraction in the summer wood of Akamatsu is shown in Fig. 7. It seems that there is a linearity between the values of the two arcs.

The mean micell angle of Akamatsu wood compared with the tracheid length from SUDO's data are shown in Fig. 8.⁵⁾ It shows clearly that the correlation be-

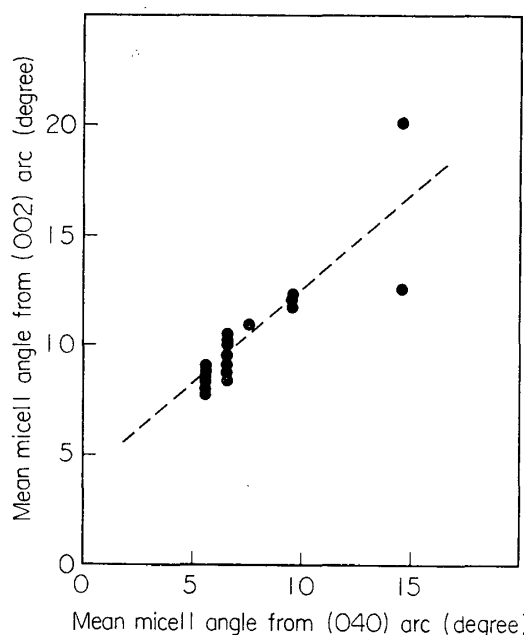


Fig. 7. Correlation between (040) mean micell angle and (002) mean micell angle.

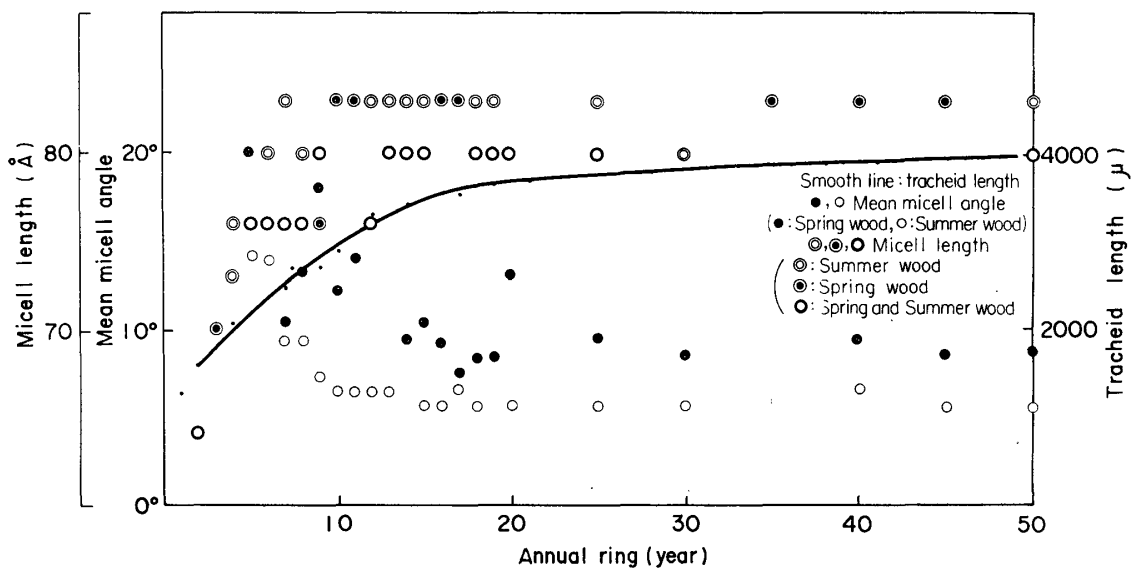


Fig. 8. Comparison with the tracheid length from Sudo's data and mean micell angle of Akamatsu wood and micell length.

tween the cell length and the micell angle was quite significant. The micell angle is dependent on the cell length, cell diameter, cell wall thickness, as well as differences of the position of the tree and its growing environment and hence the micell angle should not be deduced from the cell length alone.⁶⁾ Nevertheless, present investigation served clearly that the micell angle depends greatly on the cell length.⁶⁾

Micell width and micell length

The micell width and the micell length of Mōsō bamboo were measured for each joint of the samples (Figs. 9, 10). It is shown that the micell width in the trunk varied slightly in the outer epidermis side of a bamboo joint. On the contrary, the width varied greatly in the inner epidermis side of the bamboo joint. That is, in the part near the root, the micell width had a larger value in the inner part of the bamboo trunk and a smaller value in the upper side of the bamboo.

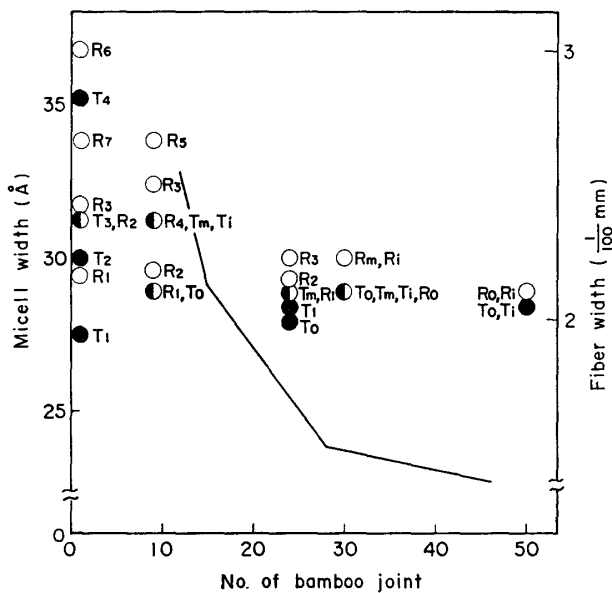


Fig. 9. Micell width of Mōsō bamboo and fiber width of Madake bamboo.

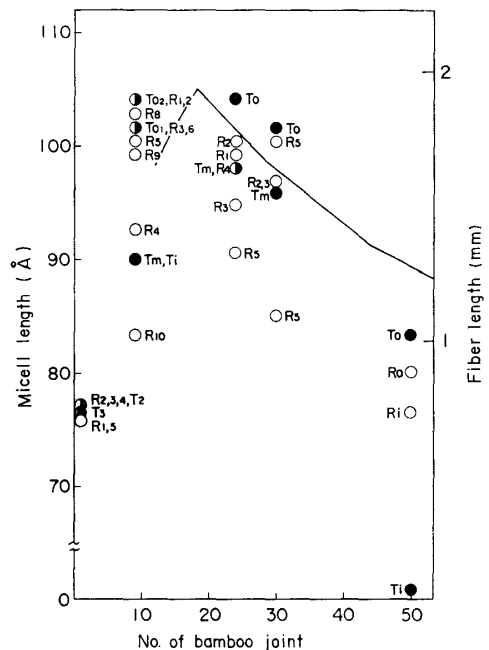


Fig. 10. Micell length of Mōsō bamboo and fiber length of Madake bamboo.

The micell length of the bamboo showed a convex upward curve when plotted against the height from the ground. Nishida, et al. measured the fiber length and the fiber width of Madake bamboo (*Phyllostachys bambusoides* SIEB. et ZUCC.).⁷⁾ and obtained similar results as shown in Figs. 9 and 10 with the smooth lines.

Figs. 11 and 12 show of the micell width and the micell length for the radial direction of Akamatsu wood. It shows that the micell width does not vary from the pith to the bark and the micell length increases outerward from the pith to

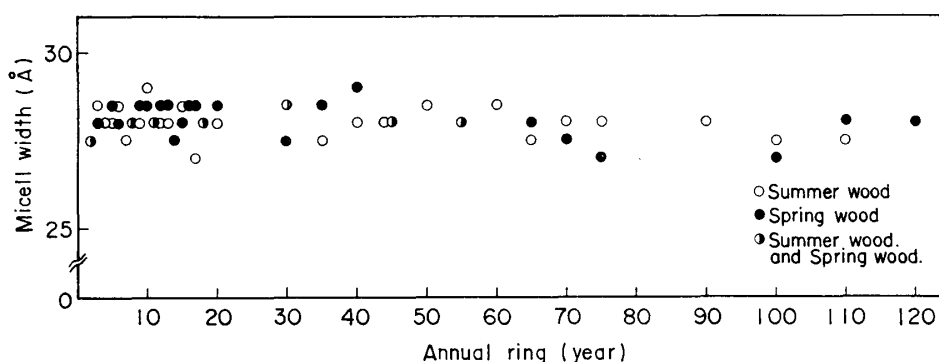


Fig. 11. Micell width of Akamatsu wood.

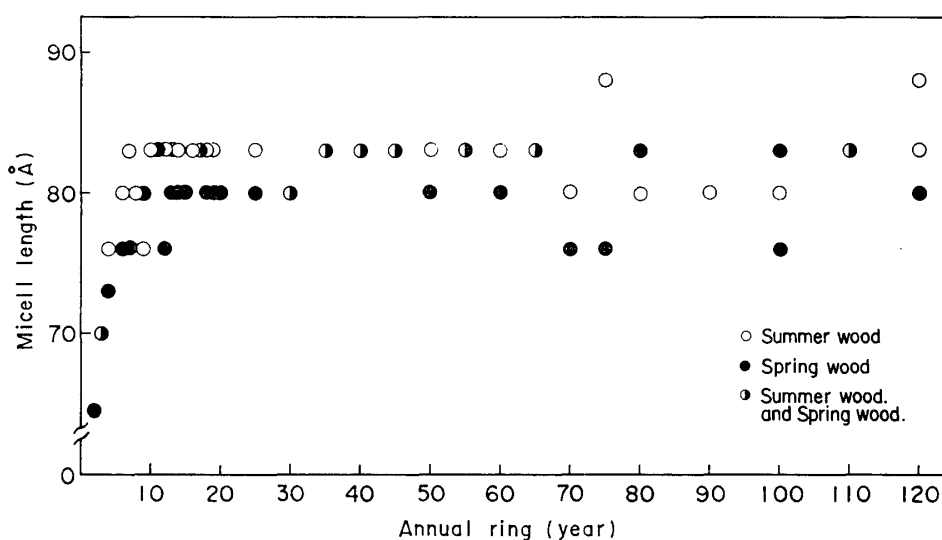


Fig. 12. Micell length of Akamatsu wood.

about 10 years toward ring and then it is a comparatively constant value near the bark. The relationship between the micell length and the mean micell angle was the same as that between the tracheid length and the mean micell angle (Fig. 8).

Degree of crystallinity

The degree of crystallinity of Mōsō bamboo is shown in Fig. 13. No significant difference was observed from the part at ground height to the top of Mōsō bamboo and the degree of crystallinity which was obtained by the following equation was about 52 %. The degree of crystallinity is obtained as follows ;

$$\text{Degree of Crystallinity} = \frac{B}{A+B} \times 100\%$$

A : The area under the amorphous curve.

B : Area of crystalline fraction.

The diffraction pattern of the amorphous fraction was measured by using edible

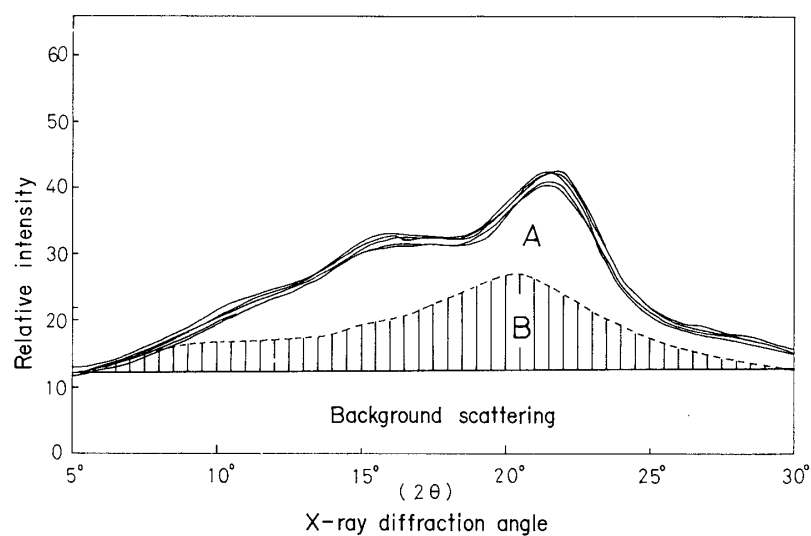


Fig. 13. X-ray diffraction curve of Mōsō bamboo
 A: crystalline region
 B: amorphous region (X-ray diffraction curve of edible shoot).

short of Mōsō bamboo, is used for the amorphous fraction.

References

- 1) M. SUZUKI, Bull. Government Forest Exp. Station., No., 212, 89 (1968).
- 2) S. WATANABE and S. INOUE, J. Chem. Soc. Japan, Indt. Chem. Section, **64**, 37 (1961).
- 3) I. D. CAVE, Forest Prod. J., **16**, 37 (1966).
- 4) P. SCHERRER, Gottinger Nachr., **2**, 98 (1918).
- 5) S. SUDO, J. Japan Wood Res. Soc., **15**, 241 (1969).
- 6) B. A. MEYLAN and M. C. PROBINE, Forest Prod. J., **19**, 30 (1969).
- 7) K. NISHIDA and K. WAKAMIYA, Cellulose Industry, **3**, 177 (1927).